UNIVERSITY *of* York

This is a repository copy of *An Overview of the IEEE P2715 Guide for the Characterization of the Shielding Effectiveness of Planar Materials*.

Article:

White Rose
university consortium
Universities of Leeds, Sheffield & York

An overview of the IEEE P2715 Guide for the characterization of the shielding effectiveness of planar materials

Adrian Suarez Zapata, *Member, IEEE*, John F Dawson, *Member, IEEE,* Yoeri Ariën, *Member, IEEE*, Johan Catrysse, *Senior Member, IEEE*, Davy Pissoort, *Senior Member,* Andrew C. Marvin , *Fellow, IEEE*,

Abstract—An electromagnetic shielding material is any material used to make shielding enclosures, typically to shield electronic components, circuits and systems against incoming electromagnetic fields, and to reduce the emission of electromagnetic waves by a circuit or system. For most applications, the choice of the material for designing and manufacturing the shielding enclosure is based on the characterization of planar samples of the shielding material. Several techniques are available to measure the shielding properties of materials. The "IEEE P2715 Guide for the characterization of the shielding effectiveness of planar materials" provides guidance on the use of recognized techniques for the measurement of planar material shielding effectiveness. The guide describes the features and limitations of commonly accepted techniques for characterizing the shielding effectiveness of planar materials, and provides a basis for comparing the techniques. This contribution introduces the P2715 standard and summarizes the methods currently available to measure the shielding provided by a planar material.

Index Terms—Electromagnetic interference, electromagnetic shielding, shielding effectiveness, characterization of planar materials, shielding effectiveness, shielding measurement

I. INTRODUCTION

THE ability to control electromagnetic interference (EMI) problems either by eliminating or by reducing coupling is of great importance. Coupling may be reduced by the use of spatial separation between the interference source and the victim circuit or the orthogonalization of them. If this is not possible or sufficient then an electromagnetic shield must be used [1]. The ideal electromagnetic shield is an infinitely conducting enclosure with no apertures or penetrations of any kind. Functional requirements and practicalities of materials, design and construction prevent this ideal from being realized. Penetrations for power, signals, and ventilation as well as access apertures for calibrations, controls, and adjustments must be incorporated into real enclosures preventing them from being an ideal shield. In many practical applications these imperfections can dominate the overall performance of a shield.

In essence, the starting point for any shield design is the performance of the material from which it is manufactured. However, the final performance of the shielding enclosure will also depend on the different aspects of the enclosure design, including its geometry, contents, apertures, the closing of different parts, the use of an appropriate gasket, etc. Due to the high variety of variables, including size and shape of the enclosures, a shielding material is normally characterized as a planar sample. Depending on the frequency range, different measurement techniques may be appropriate to cover the different parts of the frequency range of interest. The "IEEE P2715 - Guide for the characterization of the shielding effectiveness of planar materials" provides methods and procedures for determining the shielding effectiveness of planar materials such as metals, coated plastics, fiber-filled polymers, textiles, etc. The purpose of the guide is to provide guidance to the user on the selection of the appropriate test methods to determine the level of shielding provided by a material. It identifies the strengths and weaknesses of each of the recommended methods, limitations and sources of errors, and provides a basis for comparing the various techniques by providing a review of each method and its applications. In this article, we introduce the P2715 Guide and summarize all the methods it contains.

II. SHIELDING EFFECTIVENESS

Shielding materials are often based on "good conductors", that is materials with a high electrical conductivity. At low frequencies this can be complemented by a high magnetic permeability. The performance of the shield is determined both by the material from which the shield is fabricated and the structure of the shield including its size, shape, the presence of structural features such as seams, and joints, and the presence of any apertures for displays or ventilation. For shields fabricated from metal sheet the structural features are the main determinants of the shield performance as the shield material

itself is effectively opaque to electromagnetic radiation. However, the emergence of novel materials in recent years with lower conductivities than metals has seen a resurgence in the need to evaluate the shielding performance of the materials as well. This is normally done by measuring the transmission of an electromagnetic wave through a planar sample of the material. The classic description of the shielding performance of a planar sample is the Schelkunoff model [2]. The wave passing through the material is attenuated at a rate that depends on the material conductivity and permeability (skin depth). There is also reflection from the second surface of the shielding material which further reduces the energy propagating beyond the other side. Multiple reflections between the two surfaces of the materials are also possible when the attenuation in the material is small, and this can reduce the overall effectiveness of the material for shielding. The Shielding Effectiveness (SE) of the material is often defined as the ratio of the electric field strength of the wave incident on the material (E_i) to the electric field strength of the wave emerging from the far side of the material (E_t). Also the magnetic field or power density can be used. Fig. 1 illustrates an electromagnetic (EM) wave impinging on a planar material, and illustrates the three effects which together determine its SE. The model is often described in decibels as:

$$SE_{dB} = 20 \log_{10} \frac{E_i}{E_t} = A_{dB} + R_{dB} + B_{dB} \qquad (1)$$

which includes the reflection term, R that accounts for the reflection at both surfaces of the shielding material, the attenuation term A and the effect of multiple reflections (B)

For normal incidence on a shield in free space for a homogenous isotropic material the reflection term is:

$$R_{dB} = 20 \log_{10} \left(\frac{1}{1-\Gamma^2} \right) \qquad (2)$$

the absorption term is:

$$A_{dB} = 20 \log_{10} \left(e^{t/\delta} \right) \qquad (3)$$

and the multiple reflection term is

$$B_{dB} = 20 \log_{10} \left(1 - e^{-\frac{2t}{\delta}} \Gamma^2 \right) \qquad (4)$$

where:

$$\Gamma = \frac{Z_M - Z_0}{Z_M + Z_0}, \qquad (5)$$

is the reflection coefficient at the first boundary and

$$\delta = \Re \left\{ \frac{1}{\sqrt{j\omega\mu(\sigma+j\omega\epsilon)}} \right\} \approx \sqrt{\frac{2}{\omega\mu\sigma}} \qquad (6)$$

for a good conductor, is the skin depth in the shield with Z_M being the wave impedance in the shielding material:

$$Z_M = \sqrt{\frac{j\omega\mu}{j\omega\epsilon+\sigma}}, \qquad (7)$$

and Z_0 is the impedance of the incident wave. In the above ω is the angular frequency and μ, ϵ, and σ are the permeability, permittivity, and conductivity of the shielding material.
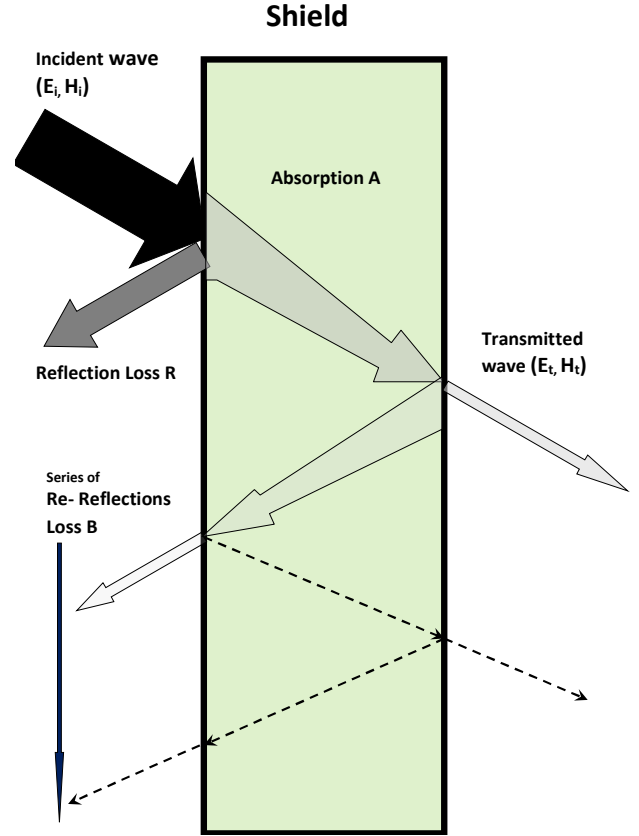

Fig. 1. Wave interaction with a planar shielding material.

In practice most of the materials measured were not simple homogenous and isotropic materials so some deviation from (1) is seen.

III. STANDARDIZED SE MEASUREMENT TECHNIQUE: ASTM D4935-18

ASTM International standard with designation D4935-18 describes the procedure and apparatus to measure directly and quantitatively the shielding effectiveness of planar materials illuminated by a far-field, normally incident electromagnetic plane wave [3]. The test fixture adopted by ASTM D4935-18 is based on the apparatus developed at the National Bureau of Standards (NBS)/ NIST and described in [4]. It was mainly designed to overcome the measurement issues arising in case of poor electrical contacts between a material under test (MUT) with high-resistivity or insulated surfaces and the metallic conductors of the coaxial cell described in the standard ASTM-ES7-83 (withdrawn in 1988).

The method lies in measuring the insertion loss (IL) that results when introducing test samples in a coaxial two-conductor transmission line holder, supporting transverse EM (TEM) propagation mode.

Fig. 2 shows the standard specimen holder. It consists of a two-port flanged coaxial cell with a constant 50 Ω characteristic impedance along its entire length and two center conductors terminating at the flange faces.
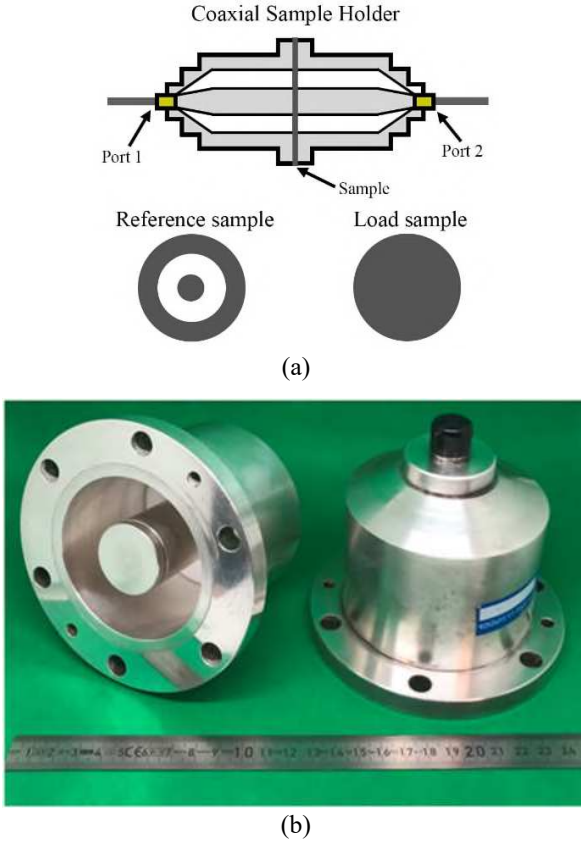
Fig. 2. ASTM D4935-18 measurement method. (a) Sketch of the typical longitudinal section of a flanged coaxial sample holder complying with ASTM D4935-18 together with load and reference specimens. (b) Two halves of a flanged coaxial sample holder for SE measurements up to 1.5 GHz.

The difference that distinguishes the ASTM D4935-18 test fixture from the one of ASTM-ES7-83 is the lack of a direct electrical contact between the metallic parts of the two halves of the coaxial cell. The interrupted inner conductor and the flanged outer one facilitate the fast mounting of the MUT between the two sections of the fixture and, more importantly allow the displacement currents to flow through an insulating material sample due to capacitive coupling. Therefore, the sample holder behaves mostly like a coaxial line with continuous inner and outer conductors. The SE evaluation procedure requires two distinct measurements involving the use of two different samples of the same MUT: the load and reference specimens. The ratio between the measurements on the reference and load specimen provides the SE of the MUT caused by reflection and absorption. The reference specimen has the same thickness of the load one. Therefore, when introduced in the cell it ensures the same discontinuity in the transmission line as when the load specimen is present but leaves empty the space in between the outer flange and inner conductor. The use of the reference specimen compensates for the effects of contact resistances and capacitive coupling between the MUT and the holder, establishing a frequency dependent reference level.

The test setup is composed of the standard fixture connected to an RF signal generator with a 50 Ω output impedance and a receiver with a 50 Ω input impedance through high quality 50 Ω matched coaxial cables. The SE of the MUT, expressed in decibels (dB) can be related to the IL in dB of the load specimen ($IL_{dB,l}$) and of the reference specimen ($IL_{dB,r}$). The SE is obtained as follows:

$$SE_{dB} = IL_{dB,l} - IL_{dB,r.} \qquad (2)$$

The standard sets the method's validity over a frequency range of 30 MHz – 1.5 GHz with a dynamic range (DR) of the order of 100 dB. This setup is limited to this frequency range because, at frequencies higher than f_c, higher-order modes other than TEM can propagate, changing the field distribution inside the cell and causing resonances which affect the measured results. Although the dominant TEM mode has no low frequency cut-off, the lower operating frequency limit is due to the discontinuous conductors and is related to the decreasing with frequency of the capacitive coupling between flanges that causes the compensation with the reference specimen to fail. This limit is not exact and can depend on the characteristics of the MUT.

IV. SE MEASUREMENT TECHNIQUES DERIVED FROM STANDARDIZED TECHNIQUES

A. ASTM D4935 – High frequency variants

Variants of the ASTM D4935-18 test fixture have been developed in order to perform SE measurements at higher frequencies and on smaller size MUTs [5]. As the cut-off frequency, and, consequently the upper frequency limit depends on cell dimensions, the new versions of 50 Ω flanged coaxial sample holders have been designed and fabricated with smaller radial dimensions to achieve a higher maximum frequency. Although the measurement procedure is analogous to that of the ASTM D4935-18, a few important aspects need to be considered. Due to the smaller cell size, the capacitive coupling can be reduced causing an increase of the value of the minimum useable frequency. Moreover, the gap discontinuity between the flanges can cause the appearance of resonances in the measured IL spectra. The frequencies of the resonances depend generally on the characteristics of the MUT and on the outer radius of the flange. These resonances cannot be canceled out from SE results by the use of the reference specimen.

B. IEEE Std 299

The IEEE Std 299 was originally issued in 1991 and is for measuring the shielding effectiveness of shielded enclosures. This document is currently dated 2006 and was reaffirmed in 2012 [6].

This method of SE measurement modifies the IEEE 299 standard by using a shielded enclosure with an aperture in which a planar sample can be mounted as shown in Fig. 3. As with the ASTM D4935-18 test fixture the Sample SE is defined as the ratio of the insertion loss between two antennas with and without the sample (2).
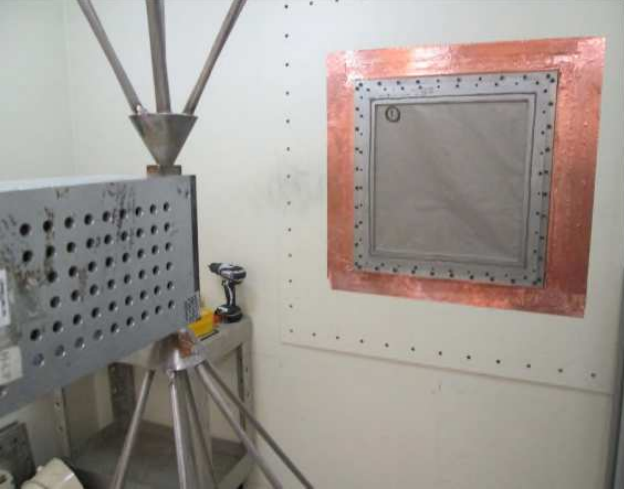
nested RC. The relationship between the energy in the outer and inner RCs allows the shielding effectiveness of the sample under test to be determined. The nested reverberation chamber method is summarized in Fig. 4.


Fig. 3. Planar sample mounted in screened room wall for SE measurement bases on IEEE Std. 299.

The reference insertion loss can either be taken in free space or through the open aperture in the shielded room wall. The sample is placed over the aperture and a second receive measurement is performed. Typically, the sample is bolted over the whole perimeter of the flange of the aperture, in order to help ensure a good contact and pressure to the shielding enclosure.

As mentioned in IEEE Std 299 the antennas used for measurement consist of loops for magnetic fields; dipoles, standard gain and ridged guide horns, biconicals, log spirals, and log periodic antennas for electric fields; and standard gain or ridged guide horn antennas for plane-wave measurements. These different antennas are needed to generate the three different types of electromagnetic fields to be measured, as well as to cover the frequency range of measurement. Linearly polarized antennas are preferred by the standard.

The IEEE 299 standard specifies a frequency range of 50 Hz to 100 GHz. However this method does not work well for planar samples when the sample is less than half a wavelength in size. In addition, one has to be aware of possible leakages due to a non-perfect clamping of the material sample and the enclosure and generating some small openings in between the sample and enclosure. This effect will typically be observed in the microwave region and can be reduced by the use of a high-performance gasket. Enclosure resonances may also affect the level of SE measured when measurements taken with different enclosures are compared.

C. Dual reverberation chambers

The reverberation chamber (RC) is able to generate an electromagnetic field which is statistically uniform and randomly polarized, when averaged over a number of samples with different stirrer positions. Dual or nested reverberations chambers can be used to measure the SE of materials. In the nested chamber method, a small chamber is located inside the larger chamber and the material under test is mounted on an aperture in the wall of the smaller chamber as described in [7] and [8]. In that way, the sample under test is exposed to a random field and the energy passing through it excites the
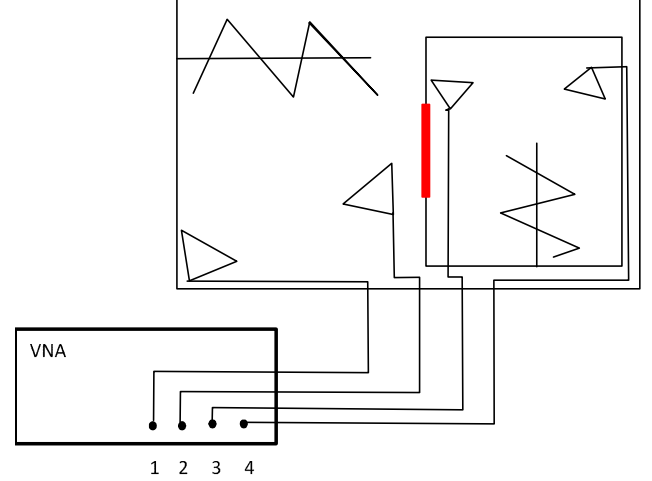
Fig. 4. The nested reverberation chamber set-up.

In Fig. 4, a four port VNA is shown connected to four antennas: a transmitting antenna (Port 1) and a receiving antenna (Port 2) in the outer chamber and a transmitting antenna (Port 3) and a receiving antenna (Port 4) in the inner chamber. The sample SE is obtained by the transmission between outer (Port 1) and inner chamber (Port 4). The presence of a receiving antenna (Port 2) in the outer chamber and of a transmitting antenna (Port 3) in the inner chamber allows the measurement of the quality factor variations in both chambers due to the sample insertion. Dual reverberation chambers, a pair of chambers joined by a common wall, may also be used in the same way. The antenna coupling measurements may also be performed using other signal sources and receivers.

Whilst solid walled chambers are often used, alternatives such as the vibrating intrinsic reverberation chamber (VIRC) shown in Fig.5 may also be used [9]. A VIRC is a reverberation chamber where the walls are made of flexible conducting material. The VIRC is mounted in a rigid structure, and connected to that structure via flexible supports. By moving the walls of the VIRC the modes will be stirred without the use of a separate mechanical stirrer. When sufficient modes are excited the EM environment will be randomly polarized, spatial uniform and isotropic.
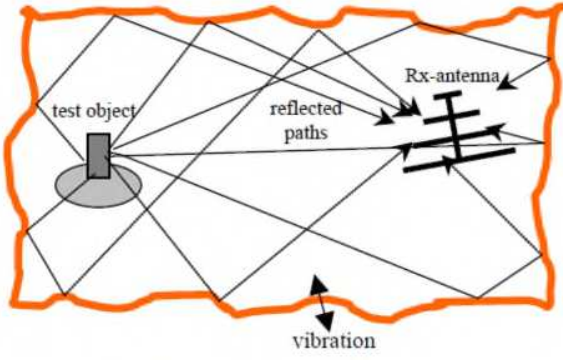
Fig. 5. Principle of a single VIRC.

A dual VIRC with solid shared wall for SE testing is shown in Fig. 6.

Fig. 6. Dual VIRC with a rigid dividing wall for SE measurement.

V. NON- STANDARDIZED SE MEASUREMENT TECHNIQUES

A. Far-field TEM-t fixture

This technique is analogous to ASTM D4935-18 in that it inserts the sample to be measured in series with a transverse electromagnetic (TEM) mode transmission line device. The type of cell has first been published by Hariya [10] from the Kansai Electronic Center for research, and it is also known as the KEC far-field test cell. The cell is shown in Fig. 7. With this technique, a square coaxial fixture is "cut" in the center, and it is constructed in such a way that both parts of the inner conductors do not any contact, not even with the sample inserted between the two halves of the cell. Coupling in and out of the test sample is capacitive. The output and input impedance of the cell is 50 Ω, and the test conditions aim to simulate far-field conditions. By varying the orientation of the test sample, its polarization dependence can be evaluated. The frequency range of operation is reported to be from 1 MHz to 1000 MHz.

Fig. 7. Far-field TEM-t fixture.

B. Near-field H-t fixture

Using the same sample of shielding material as for the TEM-t fixture, and by replacing the inner conductor by a set of small loop antennas, the near-field magnetic shielding of materials may be evaluated.

C. Dual TEM

A TEM cell is well established as a device which creates a known broad-band isolated test field. It consists of a section of rectangular coaxial transmission line tapered at each end to match 50 Ω coaxial line. The dual TEM cell shown in Fig. 8 consists of a pair of TEM cells with the added feature of an aperture in a shared wall. The aperture serves to transfer power from the driving cell (in Fig. 8: upper cell fed at Port 1) to the receiving cell (in Fig. 8: lower cell, Port 3). The MUT is placed at the aperture between the two TEM cells [11]. A comparison of the power coupled through the empty aperture to that transferred through the aperture when covered with the test material provides a relative measure of the material SE.
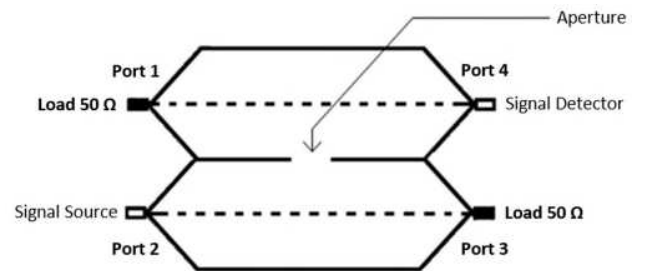

Fig. 8. Dual TEM cell with common aperture.

D. Waveguide

A sample, a rectangular piece of the material to be investigated, is inserted in a waveguide, connected to a VNA. This method relies on the principle that the waveguide carries only one mode of propagation of Transverse Electric field (TE10) in its operating band. The MUT is placed in a waveguide holder and sandwiched between two rectangular waveguide sections, which are connected to separate ports of a calibrated VNA. The VNA sends a signal down the waveguide normally incident (the dominant propagation mode being a transverse electric TE10 mode) upon the material and then the transmitted signal is measured by the VNA.
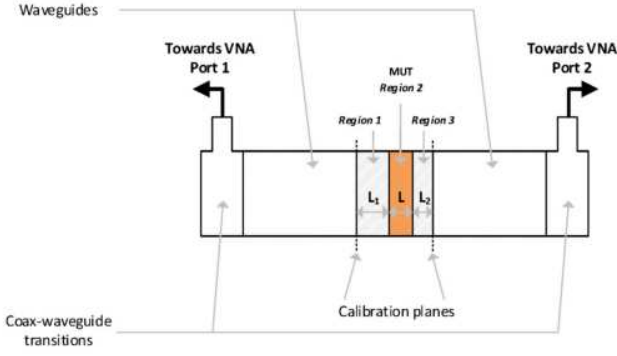
Fig. 9. Waveguide set up.

An important practical advantage of using rectangular waveguide measurements is the ease of sample manufacturing and that the sample is relatively small, compared to a free space measurement for instance. However, any gaps around the sample can result in poor accuracy.

E. Quasi optical bench

The quasi optical bench is part of the family of free-field methods. Free-fields are typically launched as diverging beams from antennas. Even if launched by a high gain antenna, the beam will typically extend beyond the aperture of the specimen allowing energy to be diffracted around the sample which reduces measurement accuracy. In focused-beam or quasi-optical methods lenses or concave mirrors are used to prevent divergence of the beam [12].

In the quasi-optical focused beam method, radiation from a corrugated horn antenna is focused using a concave elliptical mirror to produce a Gaussian beam, as shown in Fig. 10. At the beam waist the Gaussian beam is at its narrowest, and typically requires samples of 6 wavelengths in size to avoid diffraction around the sample. The SE of the sample is the ratio of the insertion loss measured between the two antenna terminals with and without the sample as in (1). This may be measured with a VNA or otherwise [12].
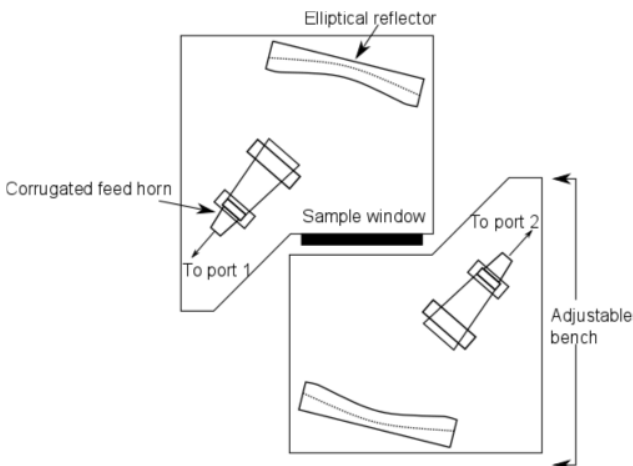

Fig. 10. Diagram of quasi-optical free space focused beam system.

The Gaussian beam method provides a relatively easy mounting and access to specimens, with clamping taking place

outside the beam waist, it has a limited influence on the result. Typical sources of uncertainties are the diffraction from specimen edges, antennas and other components; the mis-mounting of the sample if the sample is not exactly situated at the center of the beam waist; and the dynamic range limitations of the VNA.

F. Absorber box

The absorber box method, shown in Fig. 11, has been used for the shielding effectiveness SE measurement of planar samples and is described in detail in [13]. The absorber box method was conceived to overcome the problems of planar sample preparation which often affects materials with non-conductive surface (e.g. resin loaded composites, and plastics with embedded conductors). Rather than trying to assure good material contact to a metal jig which prevents energy transfer around the sample, the absorber box places the sample between two layers of Radio Absorptive Material (RAM) which prevent unwanted energy transfer.
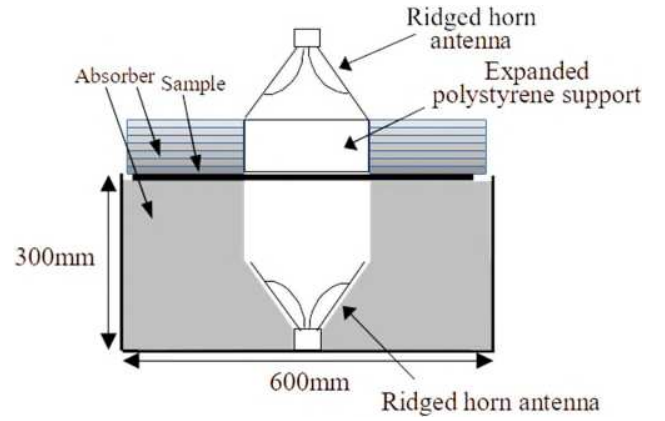

Fig. 11. Absorber box concept.

A simplistic view of the operation of the system suggests that the shielding effectiveness could be measured by taking the ratio of the transmission through the system without and with a sample present by measurement of S21 at the antenna terminals. In practice, the standing waves in the cavity between the sample and antenna cause a significant ripple on the measured SE. To minimize this effect, a reference sample technique was developed using a sample of known SE.

Using the reference sample calibration technique, the SE of the sample under test is calculated as:

$$SE_{sample} = SE_{ref} \frac{S_{21}^{ref}}{S_{21}^{sample}} \tag{3}$$

where SE_{ref} is the assumed known SE of the reference sample, S_{21}^{ref} is the measured transmission through the reference sample, an S_{21}^{sample} is the measured transmission through the sample under test.

This method has the advantages of measurement speed and lack of need for precise sample cutting an edge preparation. Samples can be inserted and removed from the system in a few seconds. The dynamic range of the measurement depends on the sample size, the greater dynamic range being obtained from

larger samples where leakage around the sample is minimized. The current implementation of the absorber box allows for samples of up to 600 mm square. The maximum measurable SE for samples of this size is in excess of 100 dB. Smaller samples need to completely cover the aperture. The two antennas are linearly polarized and so the SE is measured for the linear polarization applied to the sample. This also enables the measurement of materials with anisotropic properties.

VI. RESULTS AND DISCUSSION

The P2715 group carried out a round robin exercise where the SE of a number of planar samples was measured, using the SE measurement setups described in the previous sections. The results are summarized in this section. BAE Systems used a focused free-space measurement method with two polarizations measured. The University of York (UoY) used the Absorber Box method with two polarizations measured. Parker Chomerics used the IEEE 299 Standard method for enclosures, based on an enclosure with an aperture, with only a single x-polarized measurement. Thales used a dual VIRC method. Cisco and the Università Politecnica delle Marche (UPM) used a dual reverberation method. KU Leuven (KUL) used TEM-t and H-t methods. The University of Twente used a dual TEM and dual waveguide methods. The Wrocław University of Science and Technology (WUST), La Sapienza Università di Roma, and the University of Valencia used the coaxial transmission line method. Each method has some advantages and disadvantages and with each technique there is a range of possible associated test equipment, again the choice may depend more on budget and convenience than there being any particular best choice.

Analyzing the dynamic range is a good practice to compare the test results of the material to the dynamic range of the test set-up. The dynamic range of SE measurements is determined by several factors. First is the ratio of the transmit power of the source and the noise floor of the receiving element (instrument dynamic range), which might be considered independent of the technique used; and second is the effect of any losses in the test jig (jig loss) which reduces the measurement dynamic range from that of the instrument dynamic range by an amount equivalent to the jig loss. A third factor that can reduce the dynamic range of a measurement is the leakage of energy around the sample; this is hard to quantify as it depends on the surface condition of the sample as well as the construction of the jig and care with which it is assembled. Leakage may also occur due to coupling between cables. Fig 12. shows the dynamic range in terms of the maximum measureable SE provided by the different measurement setups defined in the P2715 guide, during the round robin. This is done by using a solid metal plate as the sample as this would be expected, according to (1), to have a SE much larger than any of the dynamic ranges shown. The coaxial and waveguide jigs have very small insertion losses so the dynamic range is essentially that of the instruments unless leakage occurs. TEM-t/H-t, Reverberation chamber, IEEE 299 absorber box and free-space methods all have significant frequency dependent insertion losses the exact details of which depend somewhat on the specific setup which means they have a dynamic range somewhat smaller than the instrumentation used. From the

results obtained in this round robin, typically, SE measurements of up to 80 dB to 90 dB are possible but in some cases the jig losses and other factors limit the maximum to much lower values.
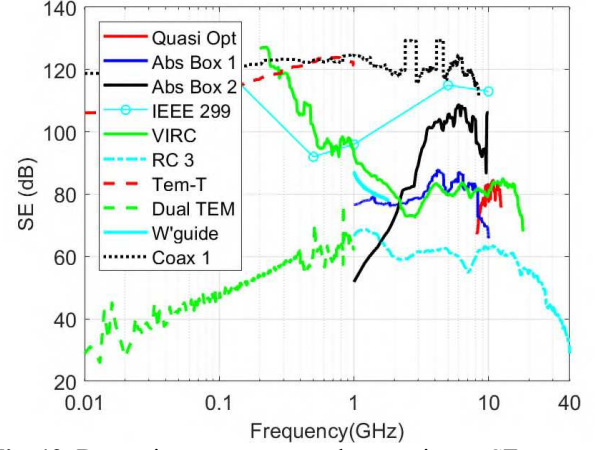

Fig. 12. Dynamic range expressed as maximum SE measurable for the different measurement setups.

Another factor to consider when selecting a SE measurement method is the frequency range which it is able to cover. The coaxial jig methods are capable in theory of working from dc up to the point where higher order modes in the jig start to cause problems, smaller jigs can be used to increase the upper frequency limit but the sample fabrication may become more difficult. In practice the low frequency limit of a coaxial jig depends on the nature of the sample. Working down to dc requires excellent connectivity between the sample and the holder, and this is difficult to achieve, particularly for the center conductor. Samples with poor surface conductivity rely on the capacitive coupling between the sample, flanges and center conductor. In this case the lower frequency depends on when the capacitive reactance becomes negligible compared to the sample impedance, though some compensation is possible [14]. The SE results obtained for a conductive fabric (Fig. 13) by comparing some coaxial jig methods based on ASTM D4935-18 procedure are shown in Fig. 14. For this material, it is possible observe a good match between the traces obtained by the different collaborators. The results from WUST Coax 0 and Coax1) show a variation of ~10 dB was measured between the SE measured using a large (100 mm diameter) and a small (18.5 mm diameter) jigs. . The results from La Sapienza, Coax 4-6 show a similar trend with decreasing jig diameter. This is believed to be due to the reduced flange area as the jig becomes smaller. .Also in Fig. 14 are plots of (1) for parameters that fit the range of measured data. Note that (1) increases steeply with frequency at the high frequency end which is representative of a homogenous material, whereas the fabric is woven as can be seen in Fig 13, The weave and small holes present tend to limit the high frequency shielding.

Fig. 13. Conductive fabric material characterized. (a) Photography of the top surface material. (b) Macro photography taken for the top surface of the material sample.
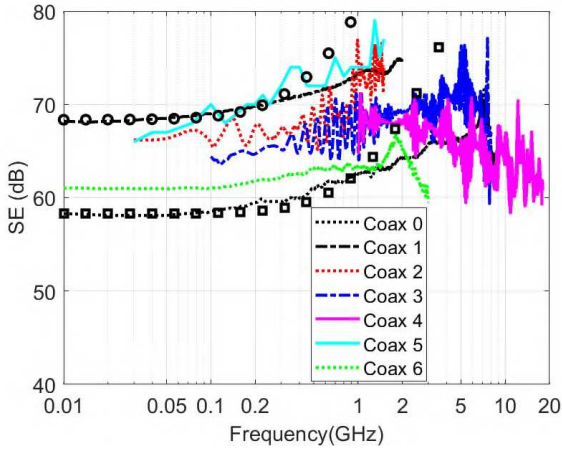

Fig. 14. SE results for the Conductive fabric, obtained with measurement methods based on the ASTM D4935-18 principle using 7 different jigs. The circular and square points are plots of (1) with conductivities of 55.6 kS/m & 12.4 kS/m and thicknesses of 0.25 mm and 0.35 mm respectively.

Most of the other methods have a lower frequency limit which depends on the physical size of the jig. Waveguide methods are restricted to the frequency range where a single waveguide mode propagates. Reverberation chamber methods are limited by the lowest useable frequency of the chamber (typically 3 times the lowest chamber resonant frequency) which depends on the chamber size and the efficacy of the stirring mechanism. The IEEE 299 method has a low frequency limit determined by the antennas and chamber used. The upper frequency for reverberation chamber and IEEE 299 methods is likely to be limited by jig and chamber leakage. The absorber box method has a low frequency limit set by the antennas used and the cutoff frequency of the absorber based waveguide (~1 GHz), and an upper limit of around 10 GHz, where higher order modes start to cause problems. In the absorber cavity these are size dependent so will change if a difference size jig is made. The free-space method is limited at the low frequency end by the antennas used and the need for the sample to be large enough to minimize edge diffraction effects (typically a number of wavelengths across). There is no obvious upper frequency limit. Fig. 15 shows the results obtained with the rest of measurement methods when the same conductive fabric material is characterized.
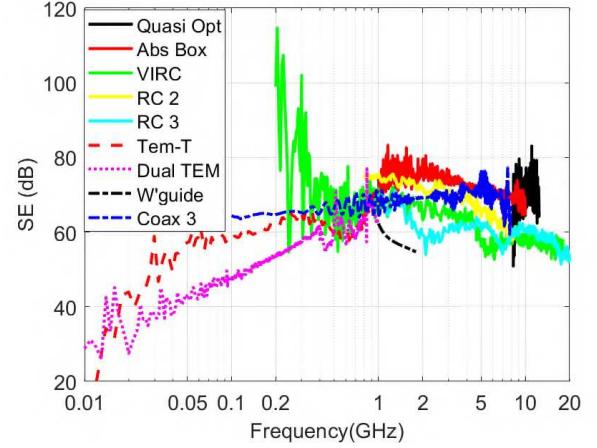

Fig. 15. SE results obtained with measurement methods different from the ASTM D4935-18 principle, with Coaxial jig 3 as a reference for comparison.

The features of the material type under test are a key factor to consider when selecting a characterization method. A major consideration with most methods is the conductivity and flatness of the sample surface where it connects to the measurement jig. If a good high-conductivity connection is not achieved many of the methods which rely on it will fail. The absorber box method is a little more tolerant of non-conducting surfaces than others, but in all cases the samples need to be flat and conform to the jig surface if leakage is to be avoided. The free space method is likely to be most tolerant of poor flatness and surface conductivity as the method does not require any connection to the material.

The coaxial method averages over all polarizations. For anisotropic materials the effect of anisotropy may not be detected with methods which inherently average over all polarizations. The Absorber box, free space, TEM-t, waveguide, and IEEE 299 methods try to illuminate the sample with a single polarization, which can reveal anisotropy if the sample is measured in two or more orientations. The reverberation chamber methods average over all polarizations and angles of incidence. Fig. 16 shows a conductive cloth material measured in the round robin and Figs. 17 and 18 show the results obtained. In this case, there is a large difference in the measurements of the ASTM and TEM-t methods with those of the reverberation chamber and absorber box. This seems to be due to the effect of a strong anisotropy of the material under test which has conducting fibers in one direction. Also the size of the ASTM jig has a substantial effect on the measured SE.
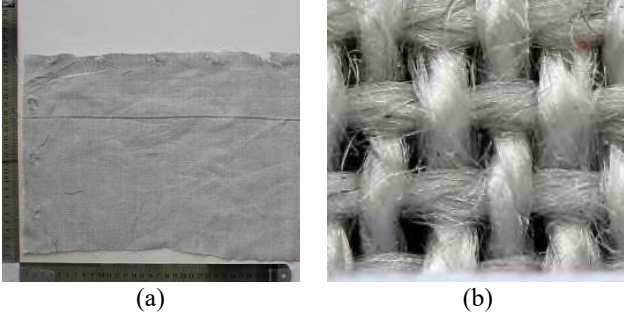
(a)   (b)

Fig. 16. Conductive cloth material characterized. (a) Photography of the top surface material. (b) Macro photography taken for the top surface of the material sample.
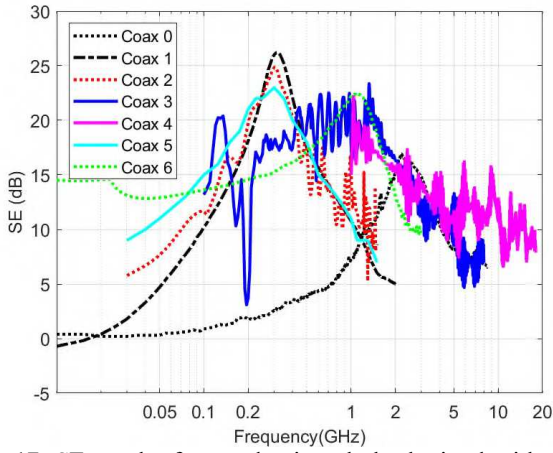

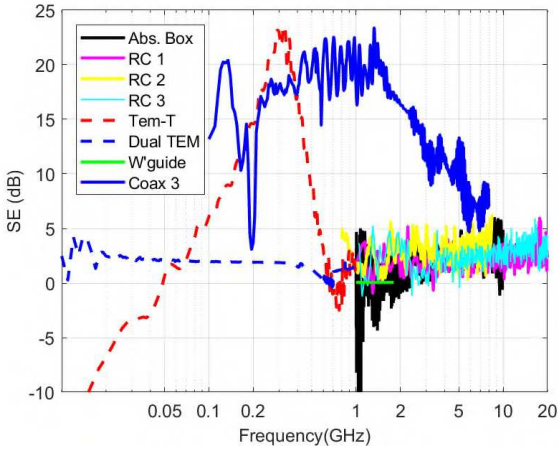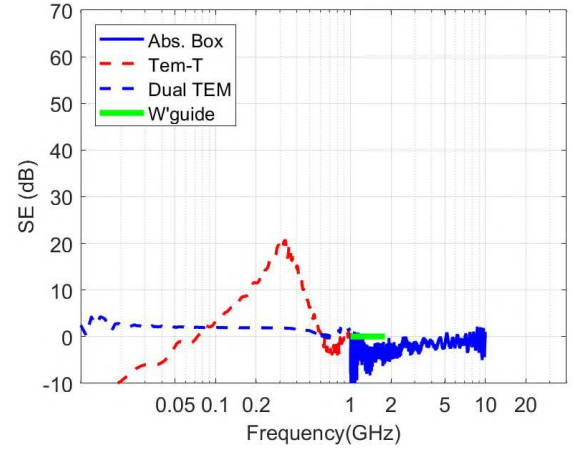**Fig. 17.** SE results for conductive cloth obtained with all the ASTM methods.
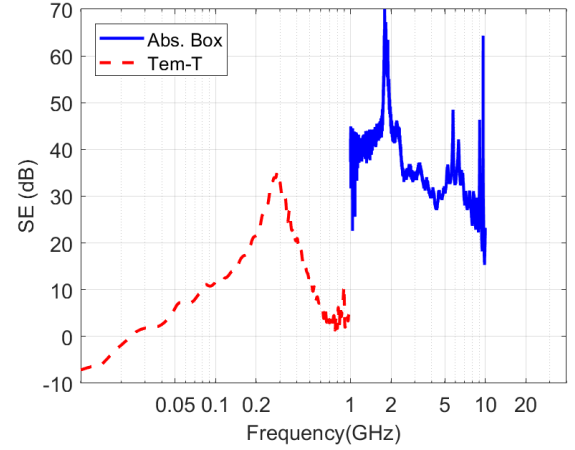

Fig. 18. SE results for conductive cloth obtained with all the ASTM methods.

As shown in Fig. 19, with some of the methods such as the Absorber Box, Tem-t, Dual TEM and Waveguide it is possible to determine the anisotropy of a material.

(a)   Conductive cloth X-polarization

(b)   Conductive cloth Y-polarization

Fig. 19. SE measurement considering two polarization positions for the conductive cloth material. (a) x-polarized SE measurements. (b) y-polarized SE measurements.

VI. CONCLUSION

All planar measurements methods exhibit variations from test to test and from sample to sample. These variations are caused by differences in test setups, normal variations in test instrumentation, differences between test samples, and aging and environmentally-induced changes in the samples. The variations between the results provided different test techniques and by different test setups can be more significant than those arising from the planar materials. Differentiating between these variations can be difficult. Test-to-test variations arise from normal differences between instruments, from differences between transmitting and receiving antennas, including their positions, and primarily from differences between test techniques.

There is no ideal technique for the measurement of SE, each method has some advantages and disadvantages and the selection of method may depend on what equipment is available as much as the other aspects below. Consequently, the P2715 guide identifies limitations and sources of errors of the commonly accepted techniques for characterizing the shielding

effectiveness of planar materials, and provides a basis for comparing the various accepted techniques.

REFERENCES

[1] E. F. Vance and W. Graf, "The role of shielding in interference control," *IEEE Transactions on Electromagnetic Compatibility*, vol. 30, no. 3, pp. 294-297, Aug. 1988, doi: 10.1109/15.3308.

[2] S. A. Schelkunoff, "Electromagnetic waves," New York, NY, USA:Van Nostrand, 1943.

[3] Standard Test Method for Measuring the Electromagnetic Shielding Effectiveness of Planar Materials, ASTM International Std. D4935-18, 2018.

[4] P. Wilson, and M. T. Ma, "A Study of Techniques for Measuring the Electromagnetic Shielding Effectiveness of Materials," *NBS Technical Note 1095*, May, 1986.

[5] A. Tamburrano, D. Desideri, A. Maschio and M. Sabrina Sarto, "Coaxial Waveguide Methods for Shielding Effectiveness Measurement of Planar Materials Up to 18 GHz," *IEEE Transactions on Electromagnetic Compatibility*, vol. 56, no. 6, pp. 1386-1395, Dec. 2014, doi: 10.1109/TEMC.2014.2329238.

[6] "IEEE Standard Method for Measuring the Effectiveness of Electromagnetic Shielding Enclosures," in *IEEE Std 299-2006 (Revision of IEEE Std 299-1997)*, pp.1-52, 28 Feb. 2007, doi: 10.1109/IEEESTD.2007.323387.

[7] C. L. Holloway, D. A. Hill, J. Ladbury, G. Koepke and R. Garzia, "Shielding effectiveness measurements of materials using nested reverberation chambers," *IEEE Transactions on Electromagnetic Compatibility*, vol. 45, no. 2, pp. 350-356, May 2003, doi: 10.1109/TEMC.2003.809117.

[8] Electromagnetic compatibility (EMC) - Part 4-21: Testing and measurement techniques - Reverberation chamber test methods, IEC Std. 61000-4-21:2011, 2011.

[9] F. B. J. Leferink, "High field strength in a large volume: the intrinsic reverberation chamber," *1998 IEEE EMC Symposium. International Symposium on Electromagnetic Compatibility. Symposium Record (Cat. No.98CH36253)*, Denver, CO, USA, 1998, pp. 24-27 vol.1, doi: 10.1109/ISEMC.1998.750054.

[10] E. Hariya and U. Masahiro, "Instruments for Measuring the Electromagnetic Shielding Effectiveness," in *1984 International Symposium on Electromagnetic Compatibility*, 1984, pp. 1-6, doi: 10.1109/ISEMC2.1984.7568140.

[11] A. Manara, "Measurement of material shielding effectiveness using a dual TEM cell and vector network analyzer," *IEEE Transactions on Electromagnetic Compatibility*, vol. 38, no. 3, pp. 327-333, Aug. 1996, doi: 10.1109/15.536062.

[12] R. N. Clarke et al., "A guide to the characterisation of dielectric materials at RF and microwave frequencies," London, UK: National Physical Laboratory, 2003.

[13] A. C. Marvin, L. Dawson, I. D. Flintoft and J. F. Dawson, "A Method for the Measurement of Shielding Effectiveness of Planar Samples Requiring No Sample Edge Preparation or Contact," *IEEE Transactions on Electromagnetic Compatibility*, vol. 51, no. 2, pp. 255-262, May 2009, doi: 10.1109/TEMC.2009.2015147.

[14] J. Catrysse, M. Delesie and W. Steenbakkers, "The influence of the test fixture on shielding effectiveness measurements," *IEEE Transactions on Electromagnetic Compatibility*, vol. 34, no. 3, pp. 348-351, Aug. 1992, doi: 10.1109/15.155853.